Non-Destructive Estimation of Mangrove Carbon for Blue Carbon Accounting in Data-Limited Regions

Aulia Lanudia Fathah
Master Program of Environmental Management & Development, Universitas Brawijaya, Kota Malang, Jawa Timur 65145, Indonesia
aulialanudiaf@gmail.com

Bambang Semedi
Master Program of Environmental Management & Development, Universitas Brawijaya, Kota Malang, Jawa Timur 65145, Indonesia
bambangsemedi@ub.ac.id

Fitri Candra Wardana
Master Program of Environmental Management & Development, Universitas Brawijaya, Kota Malang, Jawa Timur 65145, Indonesia
fitri_fia@ub.ac.id

Andik Isdianto
Department of Marine Science, Universitas Brawijaya, Kota Malang, Jawa Timur 65145, Indonesia
andik.isdianto@ub.ac.id (corresponding author)

Received: 14 June 2025 | Revised: 15 July 2025, 22 July 2025, and 28 July 2025 | Accepted: 1 August 2025

 DOI: https://doi.org/10.48084/etasr.12732

ABSTRACT

This study presented a non-destructive method for estimating mangrove biomass and carbon stock by integrating species-specific allometric equations with hemispherical canopy photography. Field surveys were conducted across 15 plots at two coastal sites in East Java - Banyuurip Mangrove Center (BMC) and Lewean Mangrove Park (LMP). Measurements of Circumference at Breast Height (CBH), tree height, and canopy images were collected, covering twelve identified species, with Avicennia marina, Rhizophora stylosa, and R. mucronata being dominant. Canopy cover was extracted from hemispherical images using ImageJ, an open-source image analysis software. Aboveground biomass ranged from 34.04 to 154.99 Mg/ha and carbon stock from 24.64 to 69.89 Mg C/ha, with canopy cover consistently above 81%. This integrated, low-cost, and scalable approach offered a replicable solution for carbon assessment in data-limited mangrove regions.

Keywords-blue carbon; mangrove forest; non-destructive biomass estimation; allometric model; hemispherical canopy analysis

I. INTRODUCTION

Climate change has caused many environmental disturbances, including sea-level rise, precipitation, and vegetation changes [1-3]. The implementation of mangrove forests as part of climate mitigation and adaptation measures includes coastal stabilization, storm surges buffering, and a major carbon sink [4, 5]. Their high above- and belowground biomass, combined with low decomposition rates in anoxic soils, makes them among the most carbon-rich ecosystems globally. As a result, mangroves are critical to blue carbon initiatives and national climate strategies.

For coastal management and reporting on climate aspects, an accurate estimation of mangrove biomass and carbon stock is important. Species-specific allometric equations that account for Diameter at Breast Height (DBH) and tree height, due to their efficiency and non-destructive nature, are widely applied [6-8]. However, carbon stock distribution is strongly determined by local environmental conditions, such as species composition, hydrology, and soil conditions [9, 10]. These variations need to be validated on-site through more adaptive methods.

Despite extensive research on mangrove carbon stocks, remote or community-managed areas have not been studies yet due to limited monitoring and data availability, which hinders their inclusion in national blue carbon MRV frameworks. Some existing studies mostly employ allometric methods, yet canopy structure is rarely taken into consideration even though it is an important factor for productivity and biomass allocation. Since canopy cover is also related to forest maturity and ecological condition, it becomes an important complementary indicator in carbon stock estimation, especially where keeping direct ground observations is difficult.

This study introduces an integrated, non-destructive method integrating species-specific allometry with hemispherical canopy photography to estimate mangrove biomass and carbon stock. This approach enhances biomass estimation in data-limited regions and supports standardized blue carbon assessments under national mitigation frameworks.

II. MATERIALS AND METHODS

A. Study Site

The research was conducted in two mangrove sites in Ujungpangkah District, East Java, Indonesia: Banyuurip Mangrove Center (BMC) and Lewean Mangrove Park (LMP), as illustrated in Figure 1. Both sites are located along the Bengawan Solo River and represent part of the North Java coastal mangrove ecosystem [9]. BMC is a community-based area restored since 2007, now functioning as an educational site restricted to research, while LMP - located further downstream - is designated as an Essential Ecosystem Area (KEE) with limited human interference [11-12].

B. Sampling Design

A total of 15 plots (10 × 10 m each) were established across five stations - three in BMC and two in LMP (Figure 2). The study followed non-destructive sampling protocols [13-14].

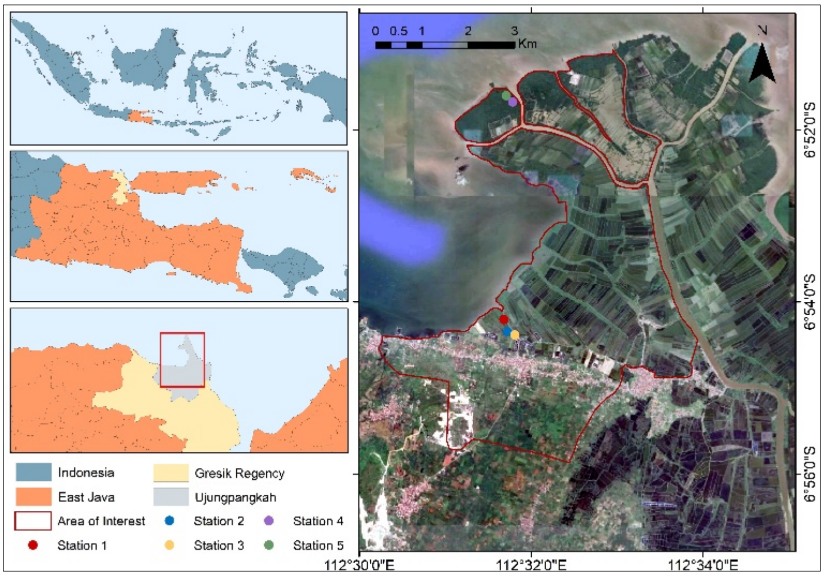

Fig. 1. Study site location.

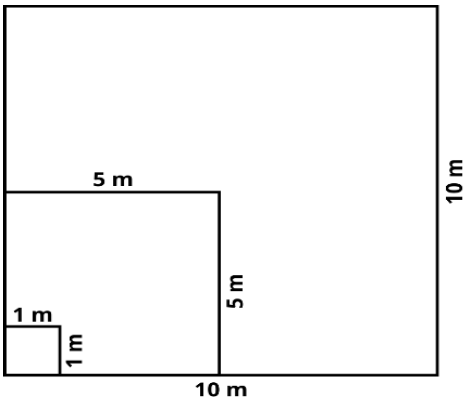

Fig. 2. Visualization of sampling plot for Mangrove.

C. Mangrove Stand Structure

All individual mangrove plants within each plot were recorded by:

- Identifying species,
- Measuring Circumference at Breast Height (CBH) at 1.3 m using a measuring tape [15],
- Measuring tree height with an Android-based clinometer or digital tools.

Species were identified based on morphological traits such as leaf shape, stem structure, and root form. When field identification was not possible, clear photographs were taken for later analysis.

CBH was converted to DBH using (1):

$$\text{DBH} = \frac{\text{CBH}}{\pi} \quad (1)$$

Individuals were classified as follows:

- Trees: DBH ≥ 4 cm,
- Saplings: DBH < 4 cm and height ≥ 1 m,
- Seedlings: height < 1 m.

1) Number of Individuals

The total number of individuals was determined by combining counts of all growth stages (trees, saplings, and seedlings) across all plots within each station.

2) Density

Species density and total density were calculated by:

$$D_i = \frac{n_i \times 10{,}000}{A} \quad (2)$$

$$D = \frac{N \times 10{,}000}{A} \quad (3)$$

where:

- D_i: Species Density (individuals/ha),
- D: Total Density (individuals/ha),
- n_i: Number of individuals of the species,
- N: Total number of individuals (all species),
- A: Total plot area (m^2),
- 10,000 is the conversion factor from m² to hectares.

The total plot area is the number of plots multiplied by area per plot (e.g., 3 plots × 100 m² = 300 m²). Figure 3 presents the flowchart of data collection and analysis of this study.

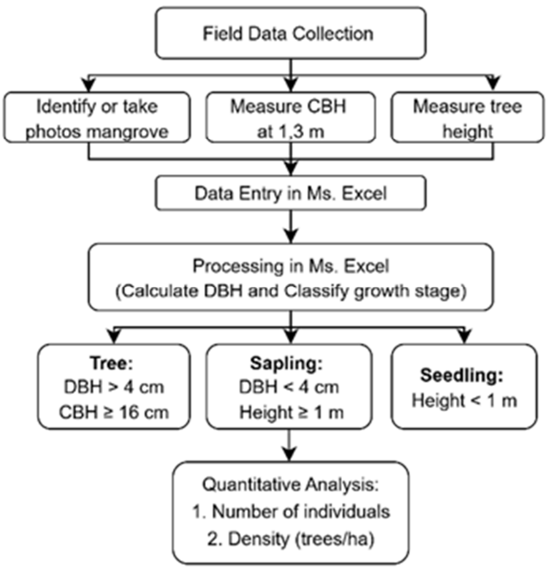

Fig. 3. Flowchart of mangrove stand structure data collection and analysis.

D. Biomass Estimation and Carbon Stocks

Biomass calculations were conducted for trees with DBH ≥ 5 cm [8] and height ≥ 1 m [16, 17]. DBH, derived from field measurements, was applied to species-specific allometric equations (Table I) [8, 18]. Wood density (ρ) values were obtained from studies (Table II) [16, 19].

Aboveground Biomass (AGB) and Belowground Biomass (BGB) were estimated per individual and summed per plot, then standardized to Mg/ha. Biomass values were converted to carbon stocks using IPCC conversion factors:

$$\text{Aboveground carbon stock} = \text{AGB} \times 0.47 \quad (4)$$

$$\text{Belowground carbon stock} = \text{BGB} \times 0.39 \quad (5)$$

The combined values yielded total vegetation carbon stock for each station. The complete analysis workflow is illustrated in Figure 4.

TABLE I. THE ALLOMETRIC EQUATIONS USED TO DETERMINE AGB-BGB

Mangrove Species	Allometric Equations
Avicennia marina	$AGB = 0.308\ DBH^{2.11*}$ $AGB = 0.1848\ DBH^{2.3524**}$ $BGB = 1.28\ D^{1.17*}$
Rhizophora apiculata	$AGB = 0.235\ DBH^{2.42*}$ $BGB = 0.00698\ D^{2.61*}$
Rhizophora stylosa	$AGB = 0.105\ DBH^{2.68*}$ $BGB = 0.261\ DBH^{1.86*}$
Rhizophora mucronata	$AGB = 0.105\ DBH^{2.68*}$ $BGB = 0.261\ DBH^{1.86**}$
Bruguiera gymnorhiza	$AGB = 0.186\ DBH^{2.31*}$ $BGB = 0.199\ \rho^{0.899} DBH^{2.22*}$
Common equations	$AGB = 0.251\ \rho\ DBH^{2.46*}$ $BGB = 0.199\ \rho^{0.899} DBH^{2.22*}$

TABLE II. MEAN VALUES OF WOOD DENSITY FOR MANGROVE SPECIES

Mangrove species	Wood density (g/cm^3)
Avicennia marina	0.732
Avicennia alba	0.600
Avicennia officinalis	0.590
Bruguiera cylindrica	0.810
Bruguiera gymnorhiza	0.741
Rhizopora apiculata	0.881
Rhizopora mucronata	0.848
Rhizopora stylosa	0.940
Sonneratia alba	0.475
Sonneratia caseolaris	0.534

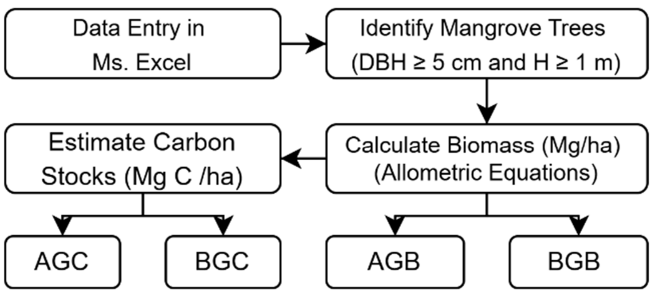

Fig. 4. Flowchart of mangrove biomass and carbon stock analysis.

E. Canopy Cover Analysis

Canopy cover was assessed using an Akaso Brave 7 action camera with a 170° wide-angle lens for hemispherical photography. Compared to DSLR or mirrorless cameras, action cameras offer practical advantages in mangrove environments, including compact size, waterproof housing, and no need for external fisheye lenses. Unlike smartphones, they provide better optical calibration and stability for quantitative canopy analysis [20].

At each 5 × 5 m plot, four hemispherical images were captured from diagonal positions at a fixed height of ~1.3 m (Figure 5). These positions were located near the corners of the plot to ensure comprehensive canopy coverage from multiple angles. Images were processed using ImageJ software: converted to 8-bit grayscale, then binarized by applying a threshold to distinguish canopy (black pixels) from sky (white pixels) [20-21]. Canopy cover percentage was computed using (6) and visualized in Excel as station-wise tables and charts (Figures 6 and 7).

$$Canopy\ Cover\ (\%) = \left(\frac{Canopy\ Pixels}{Total\ Pixels}\right) \times 100 \qquad (6)$$

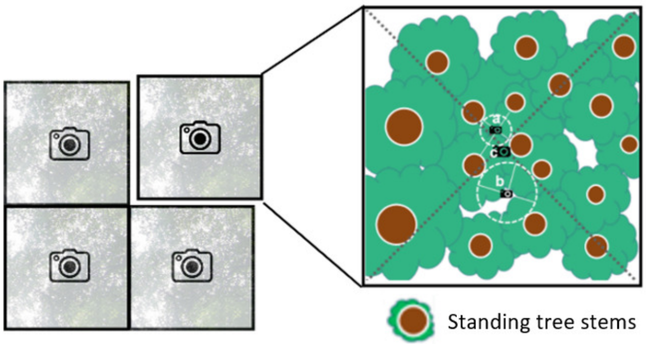

Fig. 5. Schematic layout of hemispherical photograph positions at each plot.

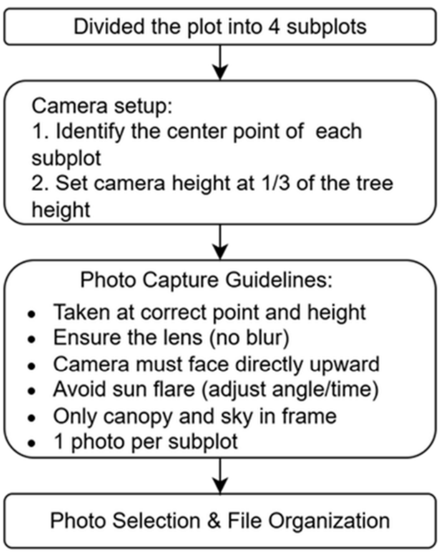

Fig. 6. Hemispherical photo capture technique.

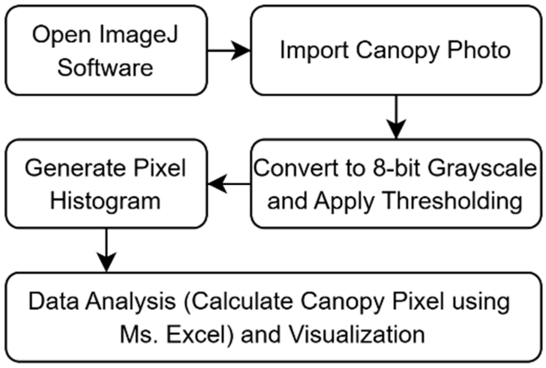

Fig. 7. Flowchart of canopy cover analysis.

All field data were processed using Microsoft Excel, and statistical summaries were compiled for analysis. The dataset used in this study is available from the corresponding author upon request.

III. RESULTS AND DISCUSSION

A. Mangrove Species Composition and Stand Structure

A total of twelve mangrove species from six genera were identified across five stations at BMC and LMP. Species identification relied on key morphological features, including leaf shape, stem characteristics, and root structure, as illustrated in Figure 8(a). CBH was measured at 1.3 m for most species, or 30 cm above the highest prop root for Rhizophora, following established protocols [15]. For trees with multiple stems at breast height, all diameters were measured and their average used as CBH and DBH values (Figures 8(b) and 8(c)).

The most dominant species was Avicennia marina, with 143 individuals, reaching the highest density at Station 1 (967 trees/ha). Other abundant species included Rhizophora mucronata (52 individuals) and R. stylosa (60 individuals), especially found in large numbers at Station 5. Rare species included Bruguiera cylindrica, Lumnitzera racemosa, and Aegiceras corniculates, each recorded only once at a single station (Table III). Avicennia (A. officinalis and A. marina) species are known for their fast growth and pioneer traits [4], [18], while R. stylosa and R. mucronata are highly adapted to specific tidal and substrate conditions [22-23].

Total tree density varied significantly, with Station 1 classified as dense (1,600 trees/ha), Station 2 as moderate (1,133 trees/ha), and Station 3 as sparse (100 trees/ha). Lower densities in Stations 3-5 may reflect higher proportions of saplings and seedlings, indicating early successional stages or regeneration zones. These spatial differences highlighted the influence of site conditions and successional dynamics on species composition and stand structure, which in turn affected biomass and carbon stock distributions.

Fig. 8. (a) Species identification based on leaf, stem, and root, (b) Measurement of tree CBH on sapling, (c) Measurement of tree CBH.

TABLE III. THE NUMBER OF INDIVIDUALS AND DENSITY

No	Species	Genus	Number of individuals					Total	Density				
			1	**2**	**3**	**4**	**5**		**1**	**2**	**3**	**4**	**5**
1	Avicennia marina	Avicennia	29	28	62	21	3	143	967	867	100	467	67
2	Avicennia officinalis	Avicennia	2	3	1	0	0	6	67	67	0	0	0
3	Avicennia alba	Avicennia	0	4	0	2	4	10	0	100	0	67	133
4	Rhizophora mucronata	Rhizophora	25	3	3	8	13	52	467	100	0	0	0
5	Rhizophora stylosa	Rhizophora	3	0	0	22	35	60	0	0	0	33	0
6	Rhizophora apiculata	Rhizophora	1	0	0	1	13	15	33	0	0	0	0
7	Sonneratia alba	Sonneratia	0	0	3	0	2	5	67	0	0	0	0
8	Sonneratia caseolaris	Sonneratia	0	0	0	1	3	4	0	0	0	0	0
9	Bruguiera gymnorhiza	Bruguiera	2	0	0	0	0	2	0	0	0	0	33
10	Bruguiera cylindrica	Bruguiera	1	0	0	0	0	1	0	0	0	0	33
11	Lumnitzera racemosa	Lumnitzera	0	0	1	0	0	1	0	0	0	0	0
12	Aegiceras corniculatum	Aegiceras	0	0	2	0	0	2	0	0	0	0	0
Total			63	38	72	55	73	301	1600	1133	100	567	267

TABLE IV. BIOMASS, CARBON STOCKS, AND CANOPY COVER

Station	Range DBH (cm)	DBH (cm)	Biomass (Mg/ha)			Carbon Stocks (Mg C/ha)			Canopy Cover (%)	Category
			AGB	BGB	TB	AGC	BGC	TVC		
1	6.05 - 23.25	13.75±5.77	118.06	36.93	154.99	55.49	14.40	69.89	81.48±4.61%	Dense
2	8.06 - 25.80	15.06±7.25	113.13	37.85	150.98	53.17	14.76	67.93	84.16±5.09%	Dense
3	7.32 - 13.69	9.55±3.59	21.42	12.62	34.04	17.92	8.97	26.89	81.35±7.56%	Dense
4	9.87 - 21.66	14.68±4.43	51.21	19.20	70.41	24.07	7.49	31.56	81.81±7.36%	Dense
5	5.41 - 19.96	10.67±4.42	38.59	16.67	55.26	18.14	6.50	24.64	81.46±10.91%	Dense

B. Biomass and Carbon Stock Distribution

Table IV summarizes DBH, Total Biomass (TB), and Total Vegetation Carbon (TVC) across five mangrove stations. The highest mean DBH values were recorded at Station 1 (13.75 ± 5.77 cm) and Station 2 (15.06 ± 7.25 cm), both in BMC. These stations also exhibited the greatest TB (154.99 and 150.98 Mg/ha) and TVC (69.89 and 67.93 Mg C/ha) values. In contrast, Station 3 (LMP) had the lowest DBH (9.55 ± 3.59 cm), TB (34.04 Mg/ha), and TVC (26.89 Mg C/ha).

These variations highlighted the impact of species, DBH, and tree density on carbon accumulation, with larger DBH strongly linked to higher biomass and carbon stocks, reflecting tree maturity [23-24]. Species such as Avicennia marina and A. officinalis, which were dominant and fast-growing, contributed significantly to the elevated values observed at BMC. However, environmental factors like substrate, salinity, and hydrodynamics also influenced carbon variation, even within the same species [16].

C. Canopy Cover and DBH Relationship

Figure 9 illustrates hemispherical images processed in ImageJ, where canopy cover was extracted using binary contrast. All stations exhibited dense canopy cover (>81%) as presented in Table IV.

(a)

(b)

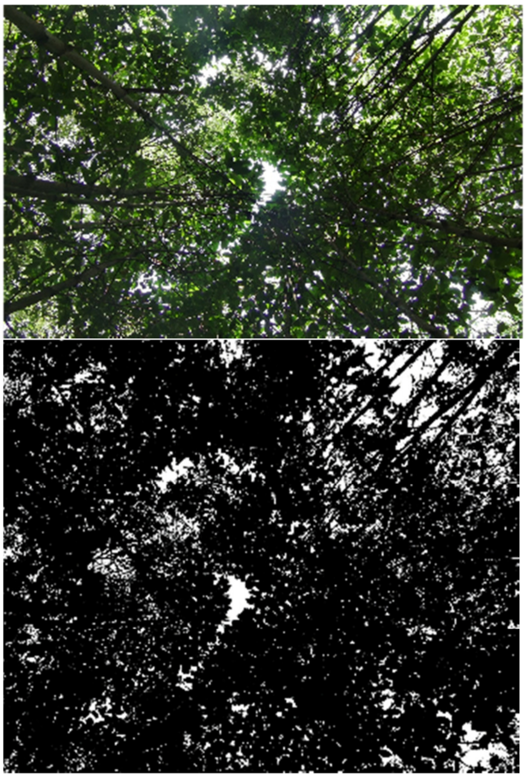

Fig. 9. Hemispherical canopy cover analysis: (a) Original hemispherical photo and (b) Thresholded binary image for canopy cover estimation using ImageJ.

Figure 10 displays the relationship between mean DBH and canopy cover. Linear regression yielded $R^2 = 0.382$ and $p = 0.266$ ($p > 0.05$), indicating a slightly positive but statistically non-significant correlation. This result aligned with other findings, who also reported a positive relationship between DBH and canopy cover [21, 25]. Station 2 (BMC) had the highest DBH (15.06 cm) and canopy cover (84.16%), while Station 3 (LMP) showed the lowest (9.55 cm and 81.35%, respectively).

These findings revealed that larger trees tended to form denser canopies, although factors such as species and substrate also played important roles. In BMC, the dominance of Avicennia marina and the presence of nutrient-rich restored mudflats, supported higher tree growth and canopy density. In contrast, LMP's natural sediments and minimal anthropogenic disturbance resulted in slower stand development. Canopy cover, when paired with allometric variables such as DBH and basal area, could also serve as a practical proxy for estimating crown volume and forest resource availability [25].

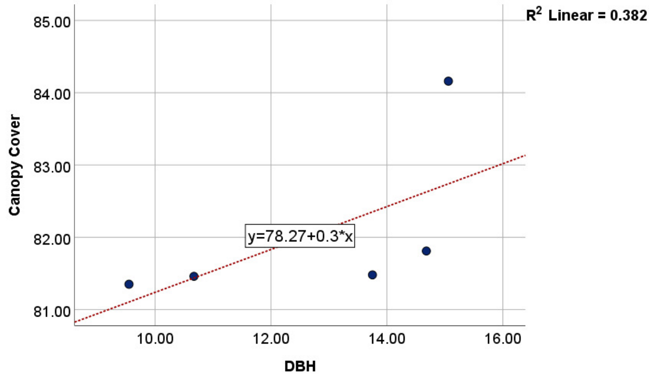

Fig. 10. Relationship between DBH and canopy cover.

This study provided a novel and practical benchmark by integrating species-specific allometry with hemispherical canopy photography, offering greater adaptability and accuracy for carbon stock assessment in data-limited mangrove regions compared to previous single-method approaches.

IV. CONCLUSION

This study proposed an integrated, non-destructive method, for the estimation of mangrove biomass and carbon stock in data-limited regions. The approach combined species-specific allometric equations - based on field measurements of Diameter at Breast Height (DBH) and tree height - with hemispherical canopy photography to capture structural attributes of the forest. Fifteen 10 × 10 plots were surveyed, from five stations, in two East Java mangrove ecosystems: Banyuurip Mangrove Center (BMC) and Lewean Mangrove Park (LMP).

Biomass ranged from 34.04 to 154.99 Mg/ha while carbon stock ranged from 24.64 to 69.89 Mg C/ha, with canopy cover always above 81%. A moderate, non – significant correlation ($R^2 = 0.382$; $p = 0.266$) between DBH and canopy cover suggested the possibility of their combined use in carbon stock estimation. Canopy cover was measured alongside DBH and height, reflecting forest structure and correlating with crown development and photosynthetic efficiency. However, site-specific structural differences may also be shaped by species dominance and substrate conditions.

The proposed method supported standardized blue carbon accounting and implementation of nature-based climate solutions, particularly in community-managed coastal areas. It aligned with national MRV (Measurement, Reporting, and Verification) frameworks and is especially relevant for tropical regions lacking long-term carbon data. Further research is encouraged to refine and validate this approach across diverse mangrove ecosystems to enhance its applicability for blue carbon monitoring and policy integration.

REFERENCES

[1] M. A. Said, "Visitors' Knowledge, Awareness, and Perception (KAP) of Climate Change in Mashar National Park, Hail-Saudi Arabia," *Engineering, Technology and Applied Science Research*, vol. 12, no. 5, pp. 9404–9408, Oct. 2022.

[2] M. Nazari Sharabian, S. Ahmad, and M. Karakouzian, "Climate Change and Eutrophication: A Short Review," *Engineering, Technology &*

Applied Science Research, vol. 8, no. 6, pp. 3668–3672, Dec. 2018, https://doi.org/10.48084/etasr.2392.

[3] R. Rudianto, V. Darmawan, A. Isdianto, and G. Bintoro, "Restoration of coastal ecosystems as an approach to the integrated mangrove ecosystem management and mitigation and adaptation to climate changes in north coast of East Java," *Journal of Coastal Conservation*, vol. 26, no. 4, July 2022,Art. no. 37, https://doi.org/10.1007/s11852-022-00865-4.

[4] J. Su, D. A. Friess, and A. Gasparatos, "A meta-analysis of the ecological and economic outcomes of mangrove restoration," *Nature Communications*, vol. 12, no. 1, Aug. 2021, Art. no. 5050, https://doi.org/10.1038/s41467-021-25349-1.

[5] D. C. Donato, J. B. Kauffman, D. Murdiyarso, S. Kurnianto, M. Stidham, and M. Kanninen, "Mangroves among the most carbon-rich forests in the tropics," *Nature Geoscience*, vol. 4, no. 5, pp. 293–297, May 2011, https://doi.org/10.1038/ngeo1123.

[6] A. Komiyama, S. Poungparn, and S. Kato, "Common allometric equations for estimating the tree weight of mangroves," *Journal of Tropical Ecology*, vol. 21, no. 4, pp. 471–477, July 2005, https://doi.org/10.1017/S0266467405002476.

[7] A. Komiyama, J. E. Ong, and S. Poungparn, "Allometry, biomass, and productivity of mangrove forests: A review," *Aquatic Botany*, vol. 89, no. 2, pp. 128–137, Aug. 2008, https://doi.org/10.1016/j.aquabot.2007.12.006.

[8] E. Indrayani, J. Kalor, M. Warpur, and B. Hamuna, "Using Allometric Equations to Estimate Mangrove Biomass and Carbon Stock in Demta Bay, Papua Province, Indonesia," *Journal of Ecological Engineering*, vol. 22, no. 5, pp. 263–271, May 2021, https://doi.org/10.12911/22998993/135945.

[9] S. Jaikishun, "Carbon storage potential of mangrove forest in Guyana," *Bonorowo Wetlands*, vol. 7, no. 1, pp. 43–54, July 2017, https://doi.org/10.13057/bonorowo/w070109.

[10] A. R. Fitrianto and A. Samsuri, "A Rural Community's Livelihood Dynamic in the maintenance of a Mangrove Area as a Tourist Destination," *ASEAN Journal of Community Engagement*, vol. 5, no. 1, pp. 105–129, July 2021, https://doi.org/10.7454/ajce.v5i1.1090.

[11] D. Yona, N. Hidayati, S. H. J. Sari, I. N. Amar, and K. W. Sesanty, "Mangrove Seedling and Planting Techniques at the Banyuurip Mangrove Center, Banyuurip Village, Ujungpangkah District, Gresik Regency," *J-Dinamika : Jurnal Pengabdian Masyarakat*, vol. 3, no. 1. Jun. 2018, https://doi.org/10.25047/j-dinamika.v3i1.744.

[12] D. Yona, D. Kurniawan, L. I. Harlyan, A. S. G. Pinilih, S. N. Khabibah, and Y. A. Julianinda, "Establishment of a Mangrove Nursery Area in Pangkahkulon Village, Gresik," *Jurnal Pengabdian Masyarakat*, vol. 4, no. 2, pp. 97–109, Oct. 2022, https://doi.org/10.31004/abdira.v2i4.219.

[13] J. Howard, S. Hoyt, K. Isensee, M. Telszewski, and E. Pidgeon, *Coastal blue carbon: methods for assessing carbon stocks and emissions factors in mangroves, tidal salt marshes, and seagrasses*. Arlington, VA, USA: Conservation International, Intergovernmental Oceanographic Commission ofUNESCO, International Union for Conservation of Nature, 2014.

[14] A. M. Arif, G. Guntur, A. B. Ricky, R. Novianti, and I. Andik, "Mangrove ecosystem C-stocks of Lamongan, Indonesia and its correlation with forest age," *Research Journal of Chemistry and Environment*, vol. 21, no. 8, pp. 1–9, Aug. 2017.

[15] J. B. Kauffman *et al.*, "Total ecosystem carbon stocks of mangroves across broad global environmental and physical gradients," *Ecological Monographs*, vol. 90, no. 2, 2020, Art. no. e01405, https://doi.org/10.1002/ecm.1405.

[16] W. N. Aye, X. Tong, and A. W. Tun, "Species Diversity, Biomass and Carbon Stock Assessment of Kanhlyashay Natural Mangrove Forest," *Forests*, vol. 13, no. 7, July 2022, Art. no. 1013¸https://doi.org/10.3390/f13071013.

[17] W. N. Aye, X. Tong, J. Li, and A. W. Tun, "Assessing the Carbon Storage Potential of a Young Mangrove Plantation in Myanmar," *Forests*, vol. 14, no. 4, Apr. 2023, Art. no. 824, https://doi.org/10.3390/f14040824.

[18] F. Sidik, N. Widagti, and H. P. Kadarisman, *Mangroves and Climate Change: A Guide for Mangrove Monitoring Stations*. Jakarta, Indonesia: Balai Riset & Observasi Laut, 2019.

[19] *Wood Density Database*, World Agroforestry. 2015, https://www.worldagroforestry.org/output/wood-density-database.

[20] I. W. E. Dharmawan, *Hemisherical Photography Analysis of Percentage Canopy Cover of Mangrove Community*, Makassar, Indonesia: Nas Media Pustaka, 2020.

[21] M. Sraun, R. Bawole, J. Marwa, A. S. Sinery, and R. L. Cabuy, "Diversity, composition, structure and canopy cover of mangrove trees in six locations along Bintuni riverbank, Bintuni Bay, West Papua, Indonesia," *Biodiversitas Journal of Biological Diversity*, vol. 23, no. 11, Nov. 2022, https://doi.org/10.13057/biodiv/d231137.

[22] K. Kalasuba *et al.*, "Red Mangrove (Rhizophora stylosa Griff.)—A Review of Its Botany, Phytochemistry, Pharmacological Activities, and Prospects," *Plants*, vol. 12, no. 11, Jan. 2023, Art. no. 2196, https://doi.org/10.3390/plants12112196.

[23] Intergovernmental Panel on Climate Change, "2006 IPCC guidelines for national greenhouse gas inventories," 2006, https://www.ipcc-nggip.iges.or.jp/meeting/pdffiles/Washington_Report.pdf.

[24] R. Rahman, N. T. Sirajuddin, F. F. Lokollo, K. Pasanea, S. N. M. Fendjalang, and M. Hulopi, "Blue carbon potential in mangrove tree stands on the coast of West Muna," *Journal of Environmental Sustainability Management*, vol. 8, no. 2, pp. 118–131, Aug. 2024, https://doi.org/10.36813/jplb.8.2.118-131.

[25] G. Brūmelis, I. Dauškane, D. Elferts, L. Strode, T. Krama, and I. Krams, "Estimates of Tree Canopy Closure and Basal Area as Proxies for Tree Crown Volume at a Stand Scale," *Forests*, vol. 11, no. 11, Nov. 2020, Art. no. 1180, https://doi.org/10.3390/f11111180.